arXiv:1612.03396v2 [cond-mat.mes-hall] 9 Jan 2017

Point-contact function of the electronphonon interaction in zirconium

N. L. Bobrov, L. F. Rybalchenko, V. V. Fisun, and A. V. Khotkevich
B.I. Verkin Institute for Low Temperature Physics and Engineering, of the National Academy of Sciences of Ukraine, prospekt Nauki, 47, Kharkov 61103, Ukraine Email address: bobrov@ilt.kharkov.ua

(Dated: January 10, 2017; Published (Fiz. Nizk. Temp., **42**, 1035 (2016)); (Low Temp. Phys., **42**, 811 (2016))

Experimental study of the electronphonon interaction (EPI) spectra of zirconium was carried out using Yansons point-contact (PC) spectroscopy. The EPI spectral function and constant were determined. Both homocontacts ($Zr-Zr$) and heterocontacts ($Zr-Cu$, $Zr-Ag$, and $Zr-Au$) were studied. No contribution by copper, silver or gold to the heterocontact spectra was detected. The positions of five phonon features of the EPI function were observed at energies 5-6, 9-11, 13-15, 18-20, and 27-29 meV. The observed diversity of the PC spectra was attributed to the anisotropy of Zr.

PACS numbers: 71.38.-k, 73.40.Jn, 74.25.Kc, 74.45.+c

I. INTRODUCTION

The spectral functions (SF) of electron-phonon interaction (EPI) (e.g., thermodynamic, Éliashberg function, transport, microcontact, etc.) are the most detailed characteristics of the electron-phonon interaction: they define the renormalization of the electron energy spectrum of metals as well as many of the most important observable properties. The SFs of EPI are related to the phonon density of states (PDS), which makes their study also important from the perspective of the crystal lattice dynamics.

To date, the experimental data on different kinds of the SF of EPI in transition metals with a complex crystal lattice are limited to point-contact (PC) spectroscopy data [1, 2] for Co, Tc, Re, Ru, and Os. Attempts to reconstruct the pointcontact EPI functions for group-IVb hcp metals - Ti, Zr and Hf - were hindered by unfavorable physical and chemical properties of these elements (rapid formation of a strong oxide layer on the surface of each of the two electrodes designed to create a pressed point contacts). In our studies we used two different approaches to overcome these technical difficulties. In the first approach, heterocontacts Zr - noble metal (Cu, Ag, Au) were created. In this case only one surface of a Zr-electrode ends up in the region of the point contact between the two electrodes. In addition, we performed forming of these heterocontacts under a current load [3]. The second approach [4] involved the use of break junctions [5], when an elongated sample with a thinning (notch) in the middle portion was first broken under liquid helium and then a contact between clean non-oxidized surfaces was established.

The aim of the present work is to obtain the point-contact EPI function and its numerical characteristics in $\alpha - Zr$ based on experimental data. Unfortunately, the utility of the theoretical calculation of the SF of EPI for Zr reported in Ref. [4] is very limited due to the fact that the calculated graphs have been presented in the coordinates of $f(\omega/\omega_{max})$ (ω_{max} is the maximum frequency of the phonon spectrum).

II. EXPERIMENTAL METHODS

The electrodes were prepared from a polycrystalline material obtained by high-vacuum melting of zirconium iodide using an electron beam gun. Polycrystalline copper, silver and gold with the resistance ratio $R_{300K}/R_{4.2K}$ of about several hundreds were also used. The electrodes measuring $1.5 \times 1.5 \times 10$ mm were spark-cut and chemically polished. They were then washed in distilled water, dried and mounted in the setup for forming microcontacts [6]. The contacts were formed using the shear method [7] with electroforming as described in detail in Ref. [3]. The optimal point-contact resistance, at which the spectra showed the maximum intensity and the minimum background, was typically about several tens of Ohms. The EPI spectra, which are proportional to the second derivative of the current-voltage characteristics (CVC), were measured using the modulation method at acoustic frequencies at 4.2 K.

III. PROCESSING OF THE MEASUREMENT DATA

The relation between the nonlinearities of the point-contact CVC in the normal state, which arise due to the inelastic scattering of electrons in the contact region, and the EPI spectrum are determined by the fundamental equation of the Yanson theory of point-contact spectroscopy. Taking into account the background term, it can be written as [2]

$$\frac{d^2I}{dV^2}(V) = -\frac{4\pi e^3}{\hbar} n(\varepsilon_F)\Omega_{\text{eff}}\langle K\rangle[g_{pc}(\omega) + B(\omega)]|_{\omega=eV/\hbar}. \quad (1)$$

Here, $d^2I/dV^2(V)$ is the voltage dependence of the second derivative of the contact CVC, $g_{pc}(\omega)$ is the point-contact EPI function, $B(\omega)$ is the background function, $n(\varepsilon_F)$ is the density of electron states at the Fermi level for a specific spin direction, e is the elementary charge, Ω_{eff} is the effective volume of the phonon generation in the contact, K is the unnormalized point-contact form factor, and the angle brackets denote averaging over the entire Fermi surface (FS). The presence of the background function reflects the fact that the second derivative of the CVC is non-zero for $eV > \hbar\Omega_{max}$, while the EPI function should be identically zero beyond the phonon spectrum edge. The quantities Ω_{eff} and $\langle K\rangle$ depend on the geometry and cleanliness of the contact, and in addition, K also depends on the orientation of the contact axis with respect to the crystallographic directions in the metal. Equation (1) can be expressed through the experimentally measurable characteristics in the form suitable for reconstructing the EPI function $g_{pc}(\omega)$ [8]:

$$g_{pc}(\omega) + B(\omega) = C\tilde{V}_2(V)V_{1,0}^{-2}R_0^{1/2}|_{V=\hbar\omega/e}. \quad (2)$$

Here, $\tilde{V}_2(V) \propto d^2I/dV^2(V)$ and $V_{1,0} \sim dV/dI$ and R_0 are the modulating voltage $V_1(V)$ and the resistance of the point contact R for $V \to 0$. The dimensional constant C is defined for the model of a clean round aperture in the approximation of the isotropic quadratic dispersion law of electrons as

$$C = -\frac{3}{8}\left(\frac{\hbar}{2\pi}\right)^{1/2} k_F v_F, \quad (3)$$

where k_F and v_F are the Fermi wave vector and the Fermi velocity, respectively. For Zr, the values of k_F and v_F were calculated from low-temperature lattice constants [9] $c/a = 5.141\ \text{Å}/3.229\ \text{Å}$ using the relation [10] $k_F = (3\pi^2 Z/\Omega)^{1/3}$, where Z is the number of conduction electrons per unit cell and Ω is the volume of the unit cell (for hcp lattice $\Omega = (\sqrt{3}/2)a^2c$). Using $Z = 1.2$ for Zr [11], we obtain $k_F = 0.915 \times 10^{-8}\ cm^{-1}$ and $v_F = 1.06 \times 10^8\ cm/s$.

Since in the experiment the voltage at the second harmonic of the modulating current was measured $V_2(V) \propto dV^2(V)/d^2I$, this dependence is recalculated into $\tilde{V}_2(V) \propto d^2I(V)/dV^2$, according to the theorem about the derivative of an inverse function. The background function in Eq. (1) was chosen as in Ref. [12]. When assessing the effective contact diameter from the resistance, it is convenient to use the Sharvin equation for the case of spherical FS and ballistic regime, written in the form

$$d = \frac{4}{ek_F}\left(\frac{\pi\hbar}{R_0}\right)^{1/2}. \quad (4)$$

IV. EXPERIMENTAL RESULTS

We studied both homocontacts $Zr - Zr$ and heterocontacts $Zr - Cu$, $Zr - Ag$, and $Zr - Au$. Despite the fact that the interpretation of the homocontact spectra is much simpler and does not involve many assumptions required for the processing of the heterocontact spectra, the use of the latter for reconstructing the EPI function in zirconium was completely justified. As for Ta contacts [3] the contribution of the noble metals is not observable in the heterocontact spectra. This is due not only to their lower intensity, but also the peculiarities of the summation of the partial contributions into the resulting spectrum of a heterocontact.

The heterocontact spectrum does not coincide with the half-sum of the contributions from the homocontact spectra of the same diameter. This is due to the fact that the point-contact form factors of metals with different momenta in the heterocontact are not equal to each other and therefore do not match the form factor of the homocontact. In a metal with a greater p_F, the relative phase volume of nonequilibrium occupied states is lower due to the reflection of electron trajectories from the interface, resulting in a relative increase of the inelastic relaxation time τ_ε, while the intensity of the PC spectrum is proportional to $d/v_F\tau_\varepsilon$.

In other words, in a heterocontact, the contribution of a metal with a lower Fermi momentum to the resultant spectrum will be greater than the half of the spectrum

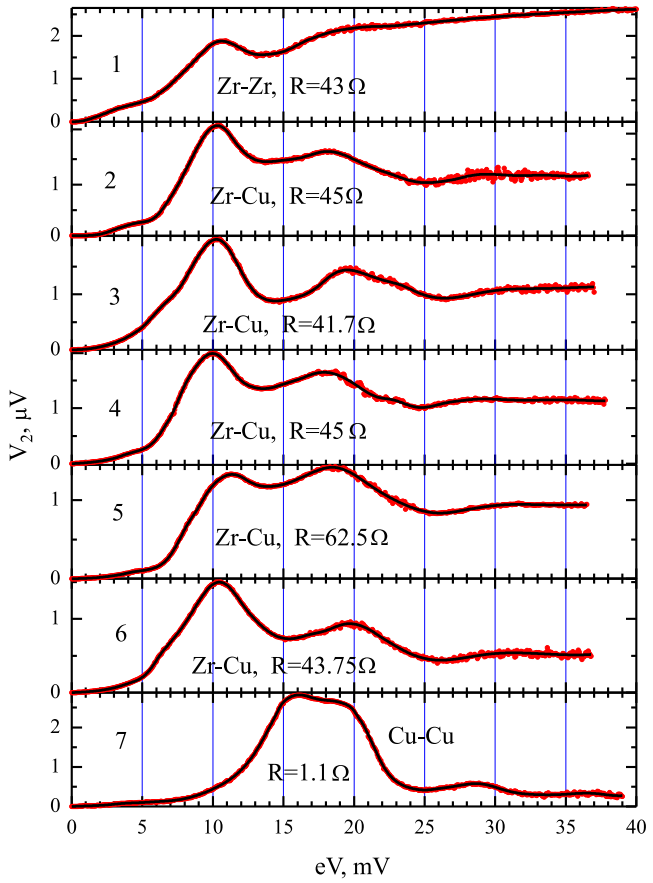

FIG. 1: Point-contact EPI spectra $V_2 \sim d^2V/dI^2$, T=4.2 K: $V_1(0)$ = 0.55(1); 0.89(2); 0.763(3); 0.878(4); 1.028(5); 1.196(6); and 0.655(7) mV.

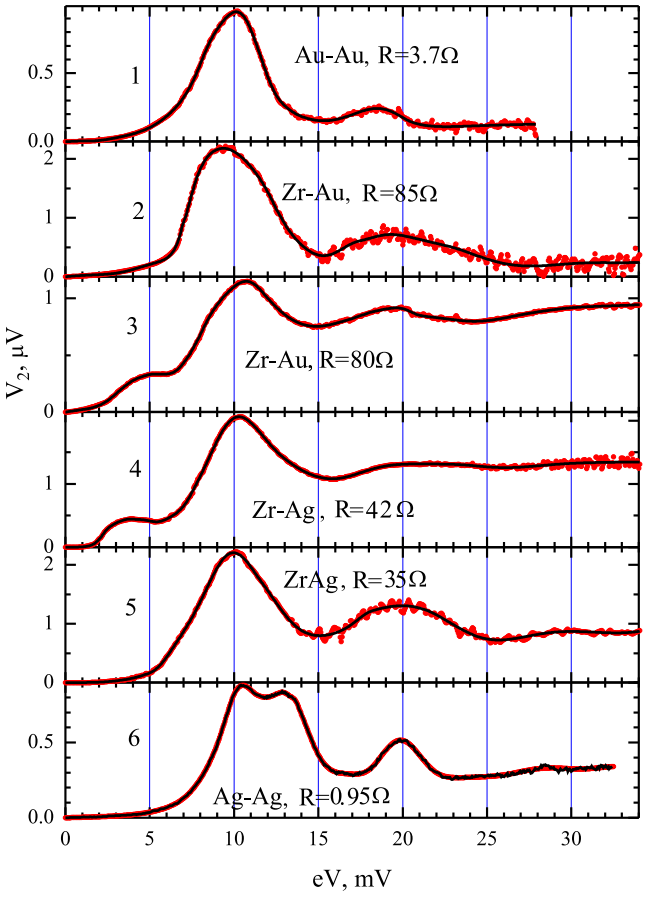

FIG. 2: Point-contact EPI spectra $V_2 \sim d^2V/dI^2$, T=4.2 K (except curve 6): $V_1(0)$ = 0.55(1); 1.213(2); 1.355(3); 0.778(4); 0.933(5) mV; curve 6 was acquired at $V_1(0)$ = 0.45 mV, $T = 1.6$ K.

corresponding to a homocontact of the same diameter; conversely, for a metal with a large momentum, it is, respectively, less.

It should be also noted that the PC spectrum of a heterocontact is symmetrical with respect to the polarity of the applied voltage, and at $T = 0$ can be represented as the sum of the PC spectra of each of the contacting metals.

The intensity ratio of the PC spectra of metals forming the heterocontact does not depend on the elastic scattering path of electrons. Introducing impurities in one metal also reduces the partial contribution to the PC spectrum of the clean one [13].

Let us estimate the expected contribution of gold to the spectrum of a $Zr - Au$ heterocontact in the free-electron approximation (due to similar Fermi parameters for Ag and Cu, the result for this pair with Zr should be similar).

As follows from Ref. [13], the intensity ratio of the partial contributions to the heterocontact spectrum is

$$L = \left(\frac{d^2I}{dV^2}\right)_1 \Big/ \left(\frac{d^2I}{dV^2}\right)_2 = \frac{v_{F_2}}{v_{F_1}} \left(\frac{p_{F_2}}{p_{F_1}}\right)^2 \frac{g_{pc}^{(1)}}{g_{pc}^{(2)}}. \quad (5)$$

Since a similar relation has been obtained in Ref. [13] for model metals with the same shape and absolute intensity of the PC function of EPI but with different Fermi velocities and momenta, the factor $g_{pc}^{(1)}/g_{pc}^{(2)}$ is absent in Ref. [13].

The absolute intensity of the PC function of EPI (Fig. 3) that we obtained for zirconium homocontacts in the freeelectron approximation for $g_{pcmax}^{Zr} = 0.34$, $g_{pcmax}^{Au} = 0.079$ [2], $v_F^{Zr} = 1.06 \times 10^8$ cm/s, $v_F^{Au} = 1.4 \times 10^8$ cm/s, $k_F^{Zr} = 0.915 \times 10^{-8}$ cm^{-1}, $k_F^{Au} = 1.21 \times 10^{-8}$ cm^{-1} yields the contribution of gold to the spectrum of the heterocontact $L_{Au} \simeq 0.1$. Note that this is the upper-bound estimate. While sufficiently large statistics has been accumulated for gold and the intensity of its EPI function

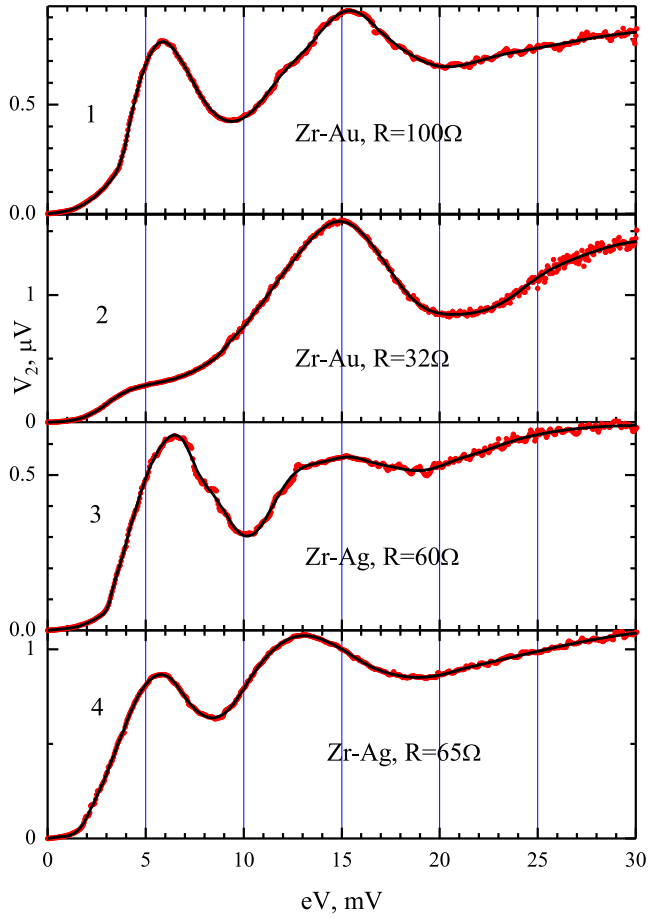

FIG. 3: Point-contact EPI spectra $V_2 \sim d^2V/dI^2$, T=4.2 K: $V_1(0) = 0.516(1)$; 1.633(2); 1.646(3); and 1.648(4) mV.

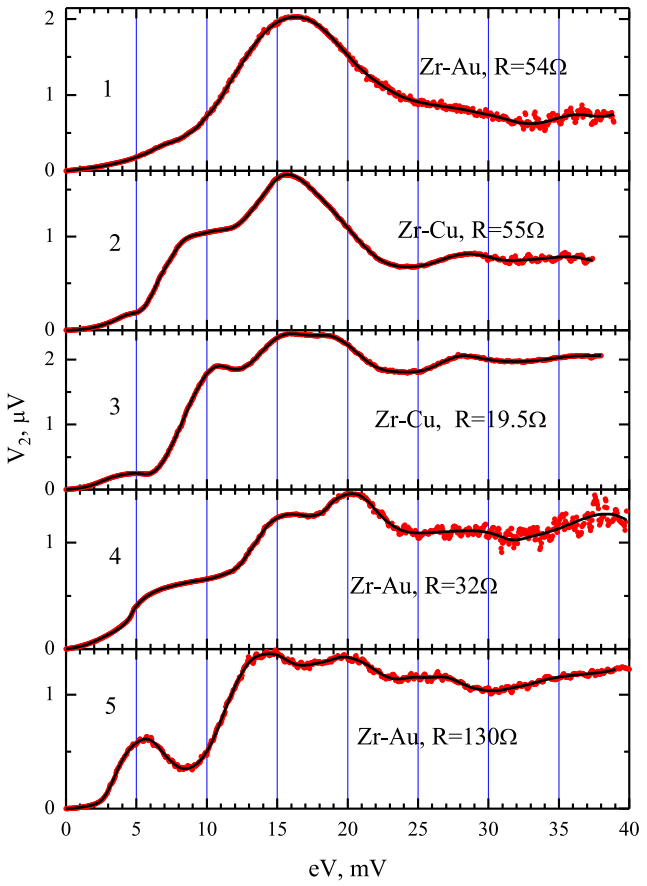

FIG. 4: Point-contact EPI spectra $V_2 \sim d^2V/dI^2$, T=4.2 K: $V_1(0) = 0.557(1)$; 1.062(2); 0.751(3); 1.06(4); and 1.777(5) mV.

has been determined with high confidence, it is not the case for *Zr*. As follows from Fig. 1, the spectrum from which the EPI function of zirconium was restored is characterized by a high level of background, which is not typical for ballistic point contacts. Thus, it is likely that an improved technology and/or the use of high-quality single crystals for the electrodes can enable obtaining more intense spectra. The importance of technology can be seen by comparing the value of the EPI function obtained in the previous study [4] using the break-junction technique with the present data. Despite the use of high-quality single crystal *Zr* for the electrodes in Ref. [4], the intensity of the EPI functions they have obtained is 9-fold lower (cf. curves 1 and 5 in Fig. 9).

The main advantage of heterocontacts is significantly higher quality of their spectra. First, the background level is several times smaller (see Fig. [1]). Second, the phonon structure is much better visible, especially in the high-frequency region. A higher yield of high-quality spectra compared to homocontacts should also be noted. Thus, for determining as accurately as possible the EPI function for many transition metals, heterocontacts with noble metal represent a preferred alternative to homocontacts.

All the obtained spectra may be divided into three groups. The most numerous group is shown in Figs. 1 and 2. As can be seen in these figures, there are two major maxima present in the spectra in the regions 9-11 and 18-20 meV. In addition, many spectra also exhibit a soft mode around $4 - 6$ meV. These figures also show the spectra of homocontacts of *Cu*, *Ag*, and *Au* for comparison. Despite the fact that some phonon features in the spectra of noble metals and *Zr* heterocontacts are sufficiently close in energy, the overall shape of the heterocontact spectra is markedly different from those of noble metals. The spectrum edge for this group is in the vicinity of 25 meV.

The second group of spectra is shown in Fig. 3. As in

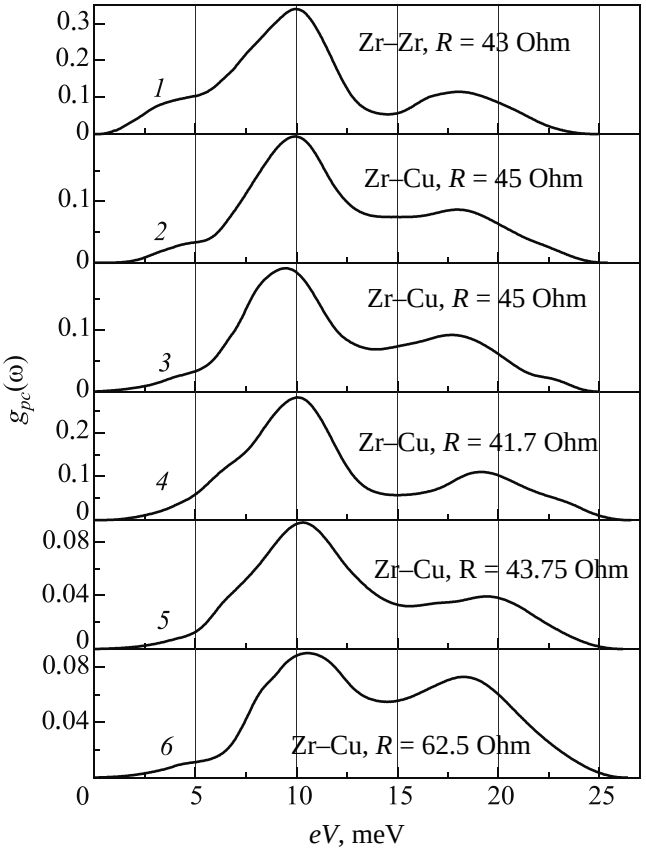

FIG. 5: Point-contact EPI function reconstructed from the spectra in Fig. 1: λ=0.66(1); 0.34(2); 0.36(3); 0.46(4); 0.16(5); and 0.18(6).

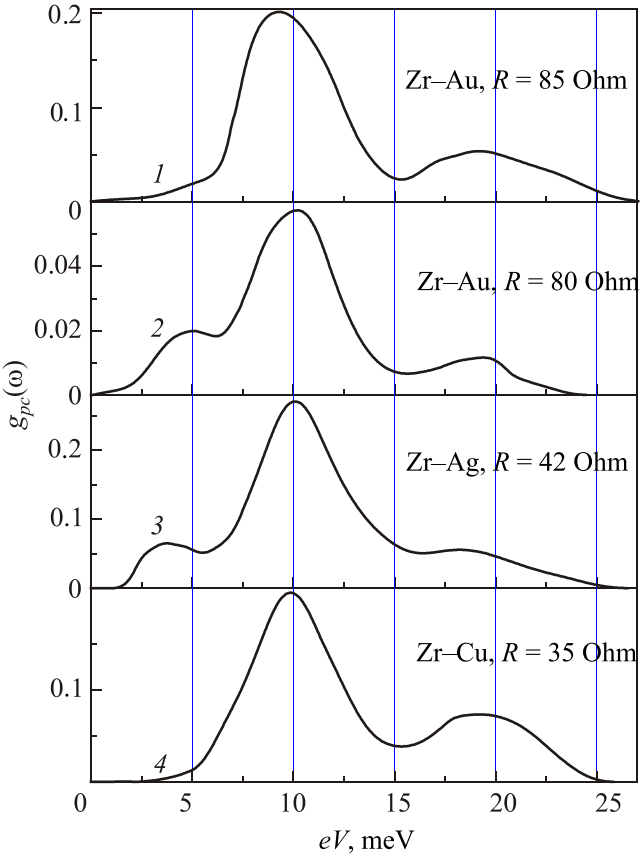

FIG. 6: Point-contact EPI function reconstructed from the spectra in Fig. 2: λ=0.295(1); 0.103(2); 0.45(3); and 0.285(4).

the previous case, there are two major maxima present in the spectra but at energies of 5-6 and 13-15 meV. There are no features in the spectra that could match the energies of those in Ag and Au, forming the heterocontacts. The spectrum edge for this group is in the vicinity of 20 meV.

The third group is presented in Fig. 4. The positions of phonon features and the shape of the spectra vary widely in this group, covering the previous cases. The hallmark of this group is the presence of a high-frequency maximum at 27-29 meV. The phonon spectrum edge is located at about 31 meV.

Figures 5, 6, 7, and 8 display the EPI functions reconstructed from the graphs in Figs. 1, 2, 3, and 4, respectively. All the values of g_{pc} and λ reported in the captions to Figs. 5-9 for the cases of heterocontacts were calculated in the same way as for the $Zr-Zr$ homocontacts of the same resistance.

In order to determine g_{pc} and λ in a Zr-heterocontact more accurately, a correction factor can be estimated:

$$K_{\rm corr} = \frac{\lambda_{pc}^{\rm get}}{\lambda_{pc}^{\rm gom}} = \frac{g_{pc}^{\rm get}}{g_{pc}^{\rm gom}} = \frac{2\,\langle K_{Zr}\rangle\, d_{Zr}}{\langle K_0\rangle\, d_{\rm get}}. \qquad (6)$$

Here $\langle K_0\rangle$ and $\langle K_{Zr}\rangle$ are the form factors for homo- and heterocontacts averaged over the Fermi surface and d_{Zr} and d_{get} are the diameters of homo- and heterocontacts, respectively. The factor 2 in the numerator is introduced to account for two-fold lower phonon generation in Zr heterocontact compared to the homocontact of the same diameter.

When calculating the diameter of the heterocontact on the zirconium side, we use the expression [3]

$$d_{\rm get} = d_{Zr}\left[2\langle\alpha_1 D\,(\alpha_1)\rangle_{V_Z>0}\right]^{-1/2}. \qquad (7)$$

Let us denote $p_{F_1}/p_{F_2} = b$ and $v_{F_1}/v_{F_2} = c$ and assume $b, c < 1$. Then

$$D(\alpha_1) = \frac{4b\alpha_1\sqrt{\alpha_1^2 + b^{-2} - 1}}{c\left(\alpha_1 + \frac{b}{c}\sqrt{\alpha_1^2 + b^{-2} - 1}\right)^2}\,, \qquad (8)$$

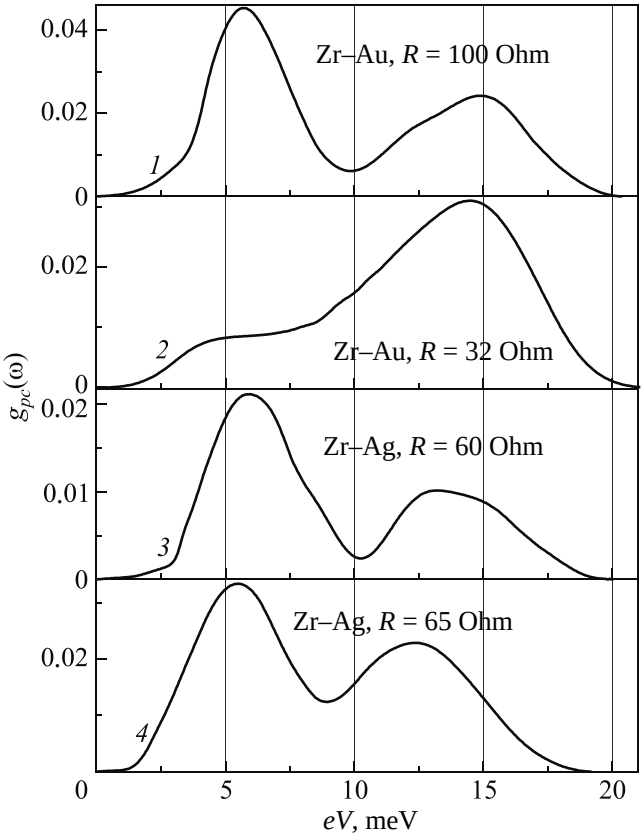

FIG. 7: Point-contact EPI function reconstructed from the spectra in Fig. 3: λ=0.085(1); 0.053(2); 0.04(3); and 0.084(4).

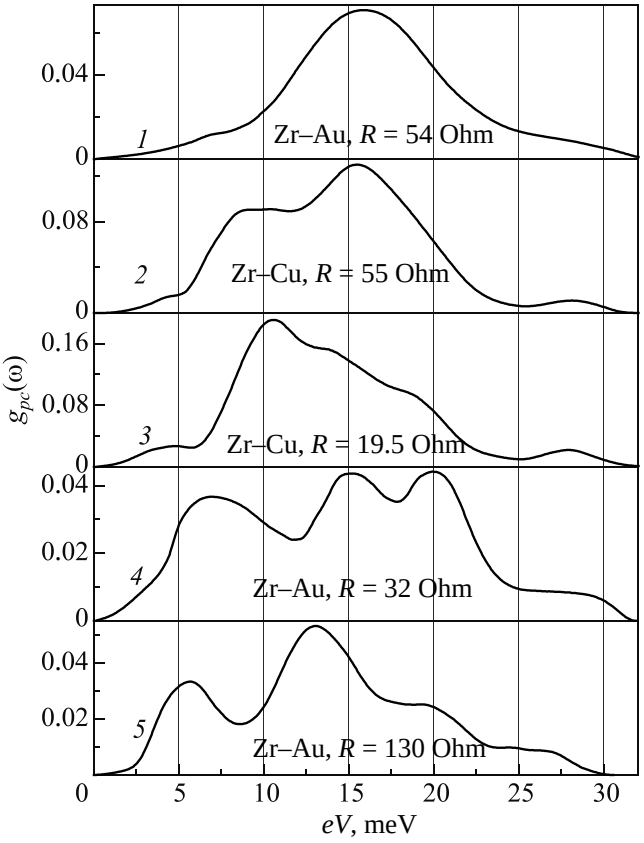

FIG. 8: Point-contact EPI function reconstructed from the spectra in Fig. 4: λ=0.115(1); 0.254(2); 0.367(3); 0.138(4); and $\lambda = 0.124(5)$.

$$2\langle\alpha_1 D(\alpha_1)\rangle_{Vz>0} = 2\int_0^1 \alpha_1 D(\alpha_1)d\alpha_1 \ . \qquad (9)$$

Now we write the expression for the form factors of a clean heterocontact [13]

$$K_s\left(\mathbf{p},\mathbf{p}'\right) = \frac{D(\mathbf{p}_s=\mathbf{p})D(\mathbf{p}_s=\mathbf{p}')}{4\langle\alpha D(\alpha)\rangle_s}K_0\left(\mathbf{p},\mathbf{p}'\right) \ , \qquad (10)$$

where $K_0(\mathbf{p},\mathbf{p}')$ are the form factors of clean homocontacts, same for both metals, and $K_s(\mathbf{p},\mathbf{p}')$ are the form factors of zirconium and the noble metal.

To determine the average form factor of zirconium heterocontacts in ballistic mode, it is first necessary to calculate the numerator of Eq. (10)

$$A_{s=Zr} = \langle D_{12}(\mathbf{p}_s=\mathbf{p})D_{12}(\mathbf{p}_s=\mathbf{p}')K_{0s}(\mathbf{p}_s,\mathbf{p}')\rangle_{V_z>0}$$

In the aperture model [13]

$$K_{0s} = K_0\left(\mathbf{p},\mathbf{p}'\right) = \frac{|v_z v'_z|\,\theta(-v_z v')}{|v_z\mathbf{v}' - v'_z\mathbf{v}|} \ , \qquad (11)$$

where θ is the Heaviside function.

For a spherical Fermi surface, after rearrangement we obtain [3]

$$A = 16\int_0^1 dx\int_0^1 dy\ \frac{xD(\alpha_1=x)D(\alpha_1=y)}{(m+n)^2}\Bigg|, \quad y>x, \qquad (12)$$

$$n = \left(1-x^2\right)^{1/4} + \left(1-x^2/y^2\right)^{1/4} \ ,$$

$$m = \left\{8\left[(1-x^2)\left(1-\frac{x^2}{y^2}\right)\right]^{1/4}\times\right.$$

$$\left.\times\left[(1-x^2)^{1/2} + \left(1-\frac{x^2}{y^2}\right)^{1/2}\right]\right\}^{1/4} .$$

Assuming $b=c=0.673$ for the couple $Zr-Cu$, we obtain $A=0.19$ and $\left[2\langle\alpha_1 D(\alpha_1)\rangle_{V_Z>0}\right]^{-1/2} = 0.86$, hence $K^{Cu}_{\rm corr} = 1.77$ For $Zr-Ag$ and $Zr-Au$ heterocontacts b

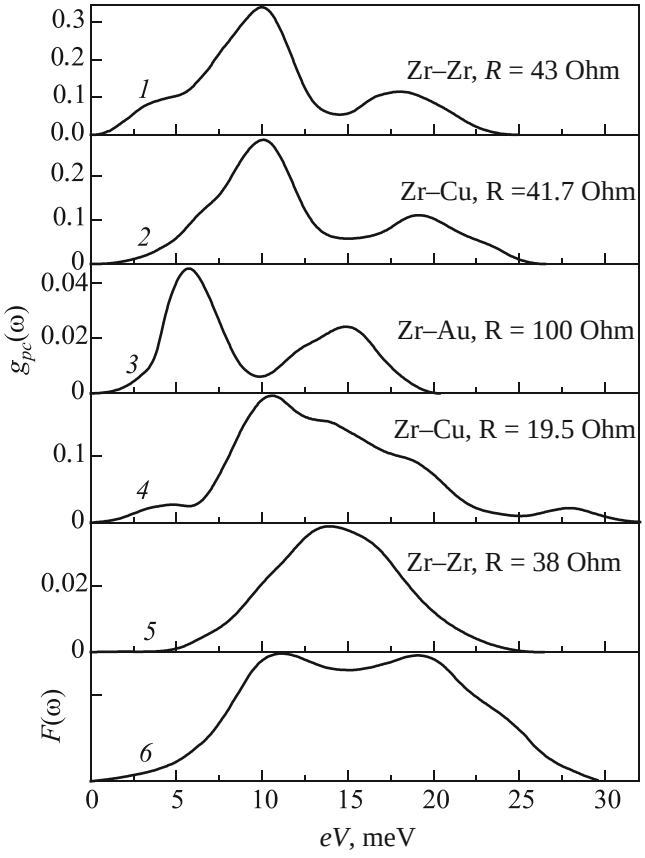

FIG. 9: Curves 1-4 are the point-contact EPI functions, selected from Figs. 5-8, which presumably correspond to different crystallographic directions: λ=0.66(1), 0.46(2), 0.085(3), and 0.367(4). Curve 5 shows the EPI function from Ref. 4 with the contact axis aligned to the crystallographic c-axis of Zr, λ=0.055. Curve 6 shows the function of the phonon density of states (data from neutron measurements [14]).

and c are approximately equal. Assuming $b = c = 0.76$, we obtain $A = 0.21$ and $\left[2\langle\alpha_1 D(\alpha_1)\rangle_{V_Z>0}\right]^{-1/2} = 0.9$, then $K_{\rm corr}^{Ag,Au} = 1.87$.

Thus, given the correction coefficients, the maximum values for the $Zr-Cu$ heterocontacts are: $\lambda = 0.81$, $g_{pc}^{\max} = 0.5$ (Fig. 5, panel 4 and Fig. 9, panel 2; $R = 41.7\ \Omega$). Accordingly, for $Zr-Ag$ we have: $\lambda = 0.84$, $g_{pc}^{\max} = 0.51$ (Fig. 6, panel 3; $R = 42\ \Omega$). Finally, for $Zr-Au$: $\lambda = 0.55$, $g_{pc}^{\max} = 0.38$ (Fig. 6, panel 1; $R = 85\ \Omega$). Recall that for the $Zr-Zr$ homocontact we obtained: $\lambda = 0.66$, $g_{pc}^{\max} = 0.34$ (Fig. 5, panel 1 and Fig. 9, panel 1; $R = 43\ \Omega$).

The fact that the refined values for the $Zr-Cu$ and $Zr-Ag$ heterocontacts turned out to be very close to each other indicate that the technological limits are reached and these contacts are apparently in the ballistic limit. Somewhat lower values for the couple $Zr-Au$ reflect the fact that a smaller number of these spectra were considered.

Thus, the use of heterocontacts allowed not only to refine the position of the phonon features in the spectra, but also to refine the value of the constant λ and the EPI function g_{pc}.

Note that this refinement factor, in addition to a spherical Fermi surface, assumes a geometrically symmetric heterocontact with a flat (mirror) boundary between the two sides. Therefore, any numerical values obtained with these coefficients are just estimates.

Finally, Fig. 9 shows all of the above types of point-contact EPI functions grouped together for clarity; they are apparently related with different orientations of the contact axis with respect to the crystallographic directions in the Zr electrode. The figure also shows the EPI function reconstructed in Ref. [4]. For the latter, it is known that the direction of the point-contact axis was aligned to the c-axis of the single crystal of Zr. Note that the EPI function (curve 1 in Fig. 8) virtually matches its shape indicating the same orientation of the contact axis. It is interesting that curve 4 in Fig. 9 includes all the five features occurring in different types of spectra. The last panel in Fig. 9 shows the function of the phonon density of states (curve 6). Unfortunately, as polycrystalline electrodes were used in the experiments, it is not possible to determine the direction of the point-contact axes. However, since most of the spectra exhibit features in the regions 9-11 and 18-20 meV, which coincides with the function of the phonon density of states, we can assume that these phonon modes dominate for the majority of the crystallographic directions.

V. SUMMARY

1. Both $Zr-Zr$ homocontacts and heterocontacts of Zr and noble metals, Cu, Ag, and Au, were employed for the experimental study of the EPI in α-zirconium using Yansons point-contact spectroscopy.

2. It was found that the contribution of noble metals to the PC spectra of $Zr-Cu$, $Zr-Ag$, $Zr-Au$ heterocontacts (second derivative of the CVCs) is not observable. In comparison with the characteristics of Zr homocontacts, the heterocontact spectra have a lower background and sharper high-frequency features.

3. From the experimental data, the graphs of the pointcontact EPI function were reconstructed, its absolute values were determined, and the value of the EPI constant was estimated. Manifestations of the anisotropy of the EPI spectrum in zirconium were observed.

The work was supported by the National Academy of Sciences of Ukraine within the Project No. FZ 3-19. The authors are grateful to Yu. G. Naydyuk for his comments and suggestions made during the discussion of the paper.

[1] I. K. Yanson, Zh. Eksp. Teor. Fiz. **66**, 1035 (1974) [Sov. Phys. JETP 39, 506 (1974)].

[2] A. V. Khotkevich and I. K. Yanson, Atlas of Point-Contact Spectra of Electron-Phonon Interactions in Metals (Kluwer Academic Publishers, Boston/Dordrecht/London, 1995).

[3] N. L. Bobrov, L. F. Rybalchenko, V. V. Fisun, and I. K. Yanson, Fiz. Nizk. Temp. **13**, 611 (1987) [Sov. J. Low Temp. Phys. **13**, 344 (1987)]; arXiv:1512.01800.

[4] V. V. Khotkevich, A. V. Khotkevich, A. P. Zhernov, T. N. Kulagina, and E. K. Folk, Bull. Khark. Natl. Karazin Univ. Ser. Phys. **476**, 96 (2000)

[5] J. Moreland and J. W. Ekin, J. Appl. Phys. **58**, 3888 (1985).

[6] N. L. Bobrov, L. F. Rybalchenko, A. V. Khotkevich, P. N. Chubov, and I. K. Yanson, Inventors Certificate 1631626 USSR, M. Kl. 5 N 01. L 21/28 (1991), Bul. no. 8.

[7] P. N. Chubov, A. I. Akimenko, and I. K. Yanson, Inventors Certificate 834803 USSR, M.Kl. 3 N. 01 L 21/28. (1981), Nul. No. 20.

[8] A. V. Khotkevich, Ph.D. dissertation, Physical and Mathematical Sciences, FTINT, Kharkov (1990).

[9] V. A. Finkel, Low-Temperature x-Ray Diffraction in Metals (Metallurgy, Moscow, 1971) [in Russian].

[10] W. A. Harrison, Solid State Theory (McGraw Hill, New York, 1970).

[11] G. Bambakidis, Phys. Status Solidi (b) **54**, K57 (1972).

[12] I. K. Yanson, I. O. Kulik, and A. G. Batrak, J. Low Temp. Phys. **42**, 527 (1981).

[13] R. I. Shekhter and I. O. Kulik, Fiz. Nizk. Temp. **9**, 46 (1983) [Sov. J. Low Temp. Phys. **9**, 22 (1983)].

[14] F. Gompf and W. Reichardt, (Progress Report of the Teilinstitut Nucleare Festkörperphysik, Fachinformationzentrum, Karlsruhe, 1975), p. 33.